J Mater Sci: Mater Med
DOI 10.1007/s10856-013-4925-2

Fumarate copolymers-based membranes overlooking future transdermal delivery devices: synthesis and properties

Magalí Pasqualone · Tamara G. Oberti · Héctor A. Andreetta · M. Susana Cortizo

Received: 8 January 2013 / Accepted: 4 April 2013

Abstract Novel copolymers of vinyl acetate and dialkyl-fumarates, poly(VA-co-DRF) with R = isopropyl (DIPF) or octan-2-yl (DOF), were synthesized by radical copolymerization under microwave conditions. The products were characterized by ^{1}H NMR and FTIR spectroscopies, size exclusion chromatography and differential scanning calorimetry. Based on these copolymers three membranes supported on polyvinyl alcohol were prepared and their morphology, swelling and mechanical properties were studied. The swelling kinetic was analyzed and interpreted in light of the Fick transport model, showing that the water transport occurs through a non-Fickian diffusion mechanism. The results show that the membrane prepared of poly(VA-co-DOF) exhibited excellent properties as potential platform for transdermal delivery system: they exhibited good tensile strength, moderated swelling and form thin and transparent films.

1 Introduction

Over the last years, an extensive research effort has been directed toward developing membranes to specific biomedical applications, such as drug delivery [1], artificial organs [2], tissue regeneration, as coating for medical devices [3], for example. In particular, the drug delivery systems have been designed to deliver a drug to a specific site, in specific time and release pattern, in order to avoid multiple doses and bypassing of the hepatic "first-pass" metabolism [4]. One of such systems is the transdermal drug delivery (TDD) whereby the drug, incorporated into a patch, is released through the skin to effect a pharmacological action at a location or locations remote from the site of action [5]. In contrast to others delivery systems, TDD is especially useful for delivery drugs which present gastrointestinal problems, such as some of those used in the treatment of bone diseases [6].

In particular, it is of interest to develop TDD applied to bisphosphonates, for which have been demonstrated significant effects as inhibitors of bone resorption mediated by osteoclasts and reversion of the deleterious actions of advanced glycation end products on osteoblastic cells [7, 8]. Despite the low oral biodisponibility of bisphosphonates, they have been developed as oral drugs [9]. The main reason for this interest is the indubitable biological efficacy of such kind of drugs. Very few bisphosphonate delivery systems have been developed. Josee et al. [10] prepared a composite material consisting of zolendronate chemically associated onto calcium phosphate and found that the release kinetic was compatible with the inhibition of bone resorption. Sodium clodronate was incorporated, at different doses, in the structure of a biomimetic calcium phosphate layer previously formed by a sodium silicate process [11]. This bisphosphonate exhibited a stimulatory effect on osteoblastic activity at low concentration. Commercial acrylic copolymers were used to design an alendronate transdermal delivery system and the effect of the inclusion of different fatty acids on the drug permeation through excised hairless mouse skin was evaluated [12]. Other transdermal delivery system of alendronate was developed using a hydrophilic patch which effectively

M. Pasqualone · T. G. Oberti · M. S. Cortizo (✉)
Instituto de Investigaciones Fisicoquímicas Teóricas y Aplicadas (INIFTA), CONICET, CCT, La Plata, Argentina
e-mail: gcortizo@inifta.unlp.edu.ar

H. A. Andreetta
Laboratorio de Farmacotécnia, Departamento Ciencias Biológicas, Facultad de Ciencias Exactas, Universidad Nacional de La Plata, 1900 La Plata, Argentina

Published online: 16 April 2013

suppressed the decrease in bone mass in model rats with osteoporosis [13].

Nam et al. [14], proposed the risedronate ion-pair formation in order to enhance the penetration of the bisphosphonate across the skin of hairless mouse. Under the studied conditions, the ion-paired risedronate proved to be 36 times more effective than risedronate alone and thus would be appropriate for a TDD.

Different kind of polymeric materials have been used for designed membranes for TDD applications, such as polyisobutilenes, polysiloxanes, acrylic copolymers [15–17]. However, in addition to its specific properties (suitable skin adhesion and cohesive strength), all of them must meet other important requirements, such as good biocompatibility with the skin, chemical compatibility with the drug and other components of the formulation and provide consistent, effective delivery of the drug [18].

Polyfumarates have been previously studied, in our group, as scaffolds for bone tissue regenerations [19]. They were able to support osteoblastic growth and was demonstrated that were biodegradable by hydrolytic and cellular mechanisms, without evidence of cytotoxicity. A compatibilized blend of poly(diisopropyl fumarate) (PDIPF) and poly(ε-caprolactone) (PCL) exhibited better surface characteristics, mechanical properties and biocompatibility than that of the homopolymer [20]. In addition, the inclusion of semi-nanohydroxyapatite in the blend, significantly improves the cell biocompatibility and osteogenicity of the scaffolds [21]. All together, these results support the hypothesis that these polymers could be useful in others biomedical applications, such as transdermal delivery systems.

In this first part of our work, we present the results of developed of a membrane suitable for a transdermal delivery system. We synthesized two new fumaric copolymers in order to compare the effect of the substituent ester on the properties of the final material. Solvent cast membranes, supported on polyvinyl alcohol (PVA), were investigated with respect to their physical aspect, morphology, water absorption capacity and mechanical properties.

2 Materials and methods

2.1 Materials

Polyvinyl alcohol (PVA, $M_w = 72{,}000$ g/mol, hydrolysis degree > 98 %), vinyl acetate (VA, 99 %), isopropyl alcohol and benzoyl peroxide (PB, recrystallized from methanol) were purchased from Merck (Buenos Aires, Argentina). 2-Octanol (97 %) and dodecylmercaptan (98 %, chain transfer agent) were purchased from Aldrich (Buenos Aires, Argentina). Fumaric acid was gifted by Maleic S.A., Argentina. Other solvents were supplied by Merck and Sintorgan (PA).

Diisopropyl fumarate (DIPF) monomer was prepared and purified as previously described [22]. Di-(octan-2-yl) fumarate (briefly: dioctyl fumarate, DOF) was synthesized by an adaptation of previous procedure carried out for DIPF. Yield, 76 %, colourless viscous liquid, n_D^{20}:1.4506. Fourier transform infrared spectra (FTIR) (ν cm^{-1}): 1,720 (C=O), 1,647 and 981 (RHC = CHR, trans), 1,258 and 1,120 (acyl–O–R). MS: m/z = 227 (M^+–C_8H_{17}), 211 (M^+–OC_8H_{17}), 183 (M^+–OC_8H_{17}–CO), 113 ($^+C_8H_{17}$).

2.2 Copolymer synthesis

Radical copolymerization of vinyl acetate (VA) with dialkyl fumarate (DRF), was carried out in bulk, initiated by BP under microwave energy, following the methodology previously reported [23]. Briefly, both monomers (VA:DRF, 75:25) together with the previously weighed mass of the initiator (40 mM) were charged into a reaction vessel and then purged with N_2 during 30 min. Reaction vessels were irradiated at 140 W during a predetermined time using a microwave oven (Zenith, ZVP-2819) of 2,450 MHz microwave frequency and 700 W maximum power. After reaching room temperature, the copolymer was isolated by methanol addition, purified by solubilization–precipitation (tolueno: methanol, or *n*-hexane:methanol, 1:5), and then dried at constant weight for conversion (C %) estimation. The copolymers of DIPF and DOF were designed as poly(VA-co-DIPF) and poly(VA-co-DOF), respectively.

2.3 Techniques of characterization

DOF monomer GC–MS analyses were done using a Perkin Elmer Clarus 560DMS–gas chromatograph equipped with a mass selective detector with quadrupole analyzer and photomultiplier detector and as split/splitless injector. In the gas chromatographic system, an Elite5MS (Perkin Elmer) capillary column (30 m, 0.25 mm ID, 0.25 μmdf) was used. Column temperature was programmed from 130 to 250 °C at a rate of 5 °C/min and 250 °C for 6 min. Injector temperature was set to 260 °C and inlet temperature was kept at 250 °C. Split injections were performed with a 10:1 split ratio. Helium carrier gas was used at a constant flow rate of 1 ml/min. In the mass spectrometer, electron ionization (EI+) mass spectra were recorded at 70 eV ionization energy in full scan mode (50–400 unit mass range). The ionization source temperature was set at 180 °C.

^{1}H NMR spectra of polymers were recorded with a Variam-200 MHz (Mercury 200) at 35 °C in $CDCl_3$. Tetramethylsilane (TMS) was used as an internal standard.

Fourier transform infrared spectra (FTIR) of the polymer films deposited onto a sodium chloride (NaCl) window were recorded on a Nicolet 380 FTIR (Thermo Electron Corporation, Madison WI, USA) between 4,000 to 400 cm^{-1} with a resolution of 4 cm^{-1} and 32 accumulated scans. The EZ-OMNIC software (EZOMNIC 7.4.127, Thermo Fisher Scientific Inc, Madison, WI, USA) was used to analyze the spectra.

The molecular weight distribution and the average molecular weights were determined by size exclusion chromatography (SEC), using a LKB-2249 instrument at 25 °C. A series of four μ-Styragel® columns, ranging in pore size 10^5, 10^4, 10^3, 100 Å, was used with chloroform as an eluent. The sample concentration was 4–5 mg/ml and the flow rate was 0.5 ml/min. The polymer was detected by the carbonylic absorption of the ester group (5.75 μm), using an infrared detector (Miram 1A Infrared Analyzer) and the calibration was done with poly(methyl methacrylate)(PMMA) standards supplied by Polymer Laboratories and Polysciences.

Glass transition temperatures (T_g) were measured using a differential scanning calorimeter (Shimadzu-TA60). Samples ($\sim$5 mg) were weighed and scanned at 10 °C/min from −30 to 150 °C under dry nitrogen (30 ml/min). Three consecutive scans were performed for each sample: heating/cooling/heating.

2.4 Membrane preparation

The membranes were prepared by an adaptation of procedure of Mukherjee et al. [24]. Briefly, first a backing foil of aluminum was attached at the bottom of a glass cylinder of 5 cm diameter, on which were applied successively a layer of polyvinyl alcohol and then a layer of the fumaric copolymer. Each layer was prepared by "casting solvent" methodology. First, 6 %w/v-solution of PVA was prepared by dissolution of the polymer in ethanol: water (10:90) at 60 °C and stirred to get clear homogeneous solutions. Next, 5 ml of the above solution was casting on the aluminum foil, as backing layer, and allowed to evaporate in an oven for 4 h at 60 °C. Finally, 5 ml of a copolymer solution in chloroform (5 %w/v) was added on the previously form PVA film and newly allowed to evaporate at room temperature. The resulting membranes were dried under vacuum until constant weight, and stored in a desiccator until use. The thickness of the membrane was measurement using a micrometer.

2.5 Membrane characterization

The surfaces of the membranes were coated with gold and their morphology was examined using scanning electron microscopy (SEM; Phillips 505, The Netherlands), with an accelerating voltage of 20 kV, and the images were analyzed using Soft Imaging System ADDAII.

2.6 Mechanical properties

The tensile properties of the membranes were determined with a universal testing machine (DigimessTC500), using force load cell ('Interface' of Arizona, USA), SM-50 N capacity, at room temperature, following the methodology previously described [21]. The dog bone-shaped specimens (50 × 18 mm^2) were tested at a rate of 5 mm/min until breaking point. Ultimate tensile stress, elastic modulus and elongation at breaking point were calculated on the basis of the generated tensile stress–strain curves. The results presented are the mean values of eight independent measurements.

2.7 Swelling study

The maximum swelling and water absorption capacity of the membranes were determined as follows [25]. The membranes were weighed (w_0) and then immersed in the phosphate-buffered saline (PBS, pH 7.4) at 37 °C. At regular intervals, the samples were removed, and after wiping the surface with paper, were weighed in the wet state (w). Then the samples were dried in vacuum overnight at room temperature and weighed in the dried state. The weight of the final dry membrane was w_d. The water content of the membrane was obtained as the difference between w, the weight of the water saturated sample and w_0, the weight of the initial dried sample. The percentage of swelling of the membrane is defined as:

$$\%S_w = \frac{100(w - w_0)}{w_0} \tag{1}$$

In order to have insights into the water transport process through the fumarate copolymer membranes, the following equation was used for analyzed the swelling process [26]:

$$\frac{W_t}{W_\infty} = kt^n \tag{2}$$

where k is a characteristic constant of the system, which depends on the structural characteristics of the polymer and its interaction with the solvent, n is the swelling exponent, which describes the mechanism of water transport into the membrane, while W_t and W_∞ represent the quantities of water absorbed at time t and at equilibrium time, respectively. In the above equation the numerical value of n provides information about the water sorption mechanism. If the rate of diffusion of penetrant is the rate limiting, $n = 0.5$ (Fickian kinetics), while value of n between 0.5 and 1.0 indicates a non-Fickian diffusion process in which the relaxation of polymer chains determines the rate

of water sorption. The limit case designed as Case II transport, where $n = 1$, correspond to a conditions which the rate of water diffusion is higher than the rate of polymer chain relaxation and rate of mass uptake is directly proportional to time [27].

The value of n and k can be obtained from the slope and intercept of the plot of $\log(W_t/W_\infty)$ versus $\log t$ from the experimental data taken until 60 % of the maximum swelling.

3 Results and discussion

3.1 Copolymer synthesis and characterization

The synthesis of vinyl acetate-dialkyl fumarate copolymers was undertaken for the purpose to obtain a material that meets the best properties for use in a TDD system. The radical polymerization under microwave conditions was choose based on the known advantage of such methodology, previously applied for other similar systems in our group [22, 23]. We demonstrated that the rate of polymerization under microwave irradiation has been significantly faster than the one under thermal conditions. The selection of the comonomers was based on prior knowledge of the properties of fumaric copolymers, such as hydrophobicity–hydrophilicity, stability and glass transition temperature [28, 29]. The structure of the obtained copolymers starting of 75:25 (VA:DRF) feed monomer compositions under microwave conditions were confirmed by FTIR and ^{1}H NMR. Figure 1a, b shows both ^{1}H NMR spectra including the structure and the peaks assignation, based on the corresponding homopolymers spectra.

Poly(VA-co-DIPF): FTIR (thin film, cm^{-1}): 2,977, 2,934, 2,870 (C–H alif), 1,732 (C=O), 1,238 and 1,106 (CO–OR). ^{1}H NMR ($CDCl_3$): δ (ppm), 1.27 (–C**H**$_3$), 1.77 (–C**H**$_2$–), 2.00 (C**H**$_3$–CO), 2.78 (–C**H**<), 4.97 (–OC**H**$(CH_3)_2$).

Poly(VA-co-DOF): FTIR (thin film, cm^{-1}): 2,954, 2,930 y 2,858 (C–H), 1,737 (C=O), 1,228 y 1,116 (CO–OR).^{1}H NMR ($CDCl_3$): δ (ppm), 0.88 (–CH_2–C**H**$_3$), 1.28 (C**H**$_3$–CH–O–), 1.45–1.74 (–(C**H**$_2$)$_5$–), 1.99 (C**H**$_3$–CO), 2.66-2.92 (–C**H**<), 4.84 (–OC**H**(CH_3)–).

An alternating composition for poly(VA-co-DIPF) was demonstrated based on the reactivity ratios previously reported [30]. Although the reactivity ratios data for poly(VA-co-DOF) have not been determined yet, here too we expect an alternating monomer distribution, according to other similar systems [28].

Composition of poly(VA-co-DIPF) was estimated from the integral ratio of the peak at 1.27 ppm corresponding to methyl hydrogen (CH_3) of DIPF unit and the peaks between 1.4 and 2.0 ppm corresponding to methylene and methyl hydrogen (CH_2 and CH_3) of VA unit, using the following ratio:

$$F_{\mathrm{DIPF}} = \frac{I_1/12}{I_1/12 + I_2/5} \tag{3}$$

where F_{DIPF} is the mole fraction of DIPF in the copolymer and I_1 and I_2 represent the ^{1}H NMR resonance peak areas at 1.27 ppm and near to 1.7 ppm, respectively.

Composition of poly(VA-co-DOF) was estimated from the integral ratio of the peak at 0.88 and 1.99 ppm corresponding to the terminal methyl hydrogen of DOF unit and to the methyl hydrogen of VA unit, respectively, using the following ratio:

$$F_{\mathrm{DOF}} = \frac{I_3/2}{I_3/2 + I_4} \tag{4}$$

Where F_{DOF} is the mole fraction of DOF in the copolymer and I_3 and I_4 represent the ^{1}H NMR resonance peak areas at 0.88 ppm and near to 1.99 ppm, respectively.

Table 1 summarizes the reaction conditions, percentage of conversion, copolymer compositions (F_{DRF}), and the properties of the obtained copolymer. All the obtained copolymers present similar composition, suggesting that the both fumaric monomers exhibited the same behavior of copolymerization [28].

In order to evaluate the effect of the average molecular weight on the final properties of the membrane, two copolymers of DOF were synthesized. Although the conversion was higher for the copolymer obtained starting of DIPF than for the copolymers based on DOF, the polymerization of DIPF not produced gel fraction, which itself was obtained for the case of DOF copolymers. This observation together with the highest polydispersity index found in the molecular weight distribution of poly(VA-co-DOF), indicated that the chain transfer reaction was the predominant termination mechanism of the radical polymerization of VA with DOF. The gel fraction is produced by chain transfer reaction from the growing macroradical to polymer that involves abstraction of hydrogen atoms via H-abstraction from both backbone tertiary C–H bonds and alkyl side groups (Fig. 2), as was demonstrated by others researches through NMR studies of different systems [31, 32]. In our case, is greatest susceptibility to abstraction of tertiary compared to secondary or primary CH hydrogen atoms on the ester side group to give the branch structure and finally cross-link structures (gel fraction) by radical combination reactions.

It was reported that the addition of a chain transfer agent (CTA) did not affect the polymerization kinetics, but the molecular weights strongly decreased and gel formation was avoided [33]. Under our experimental conditions, by addition of CTA decreases of the M_w and an increase in the polydispersity index were observed. The increase of PDI

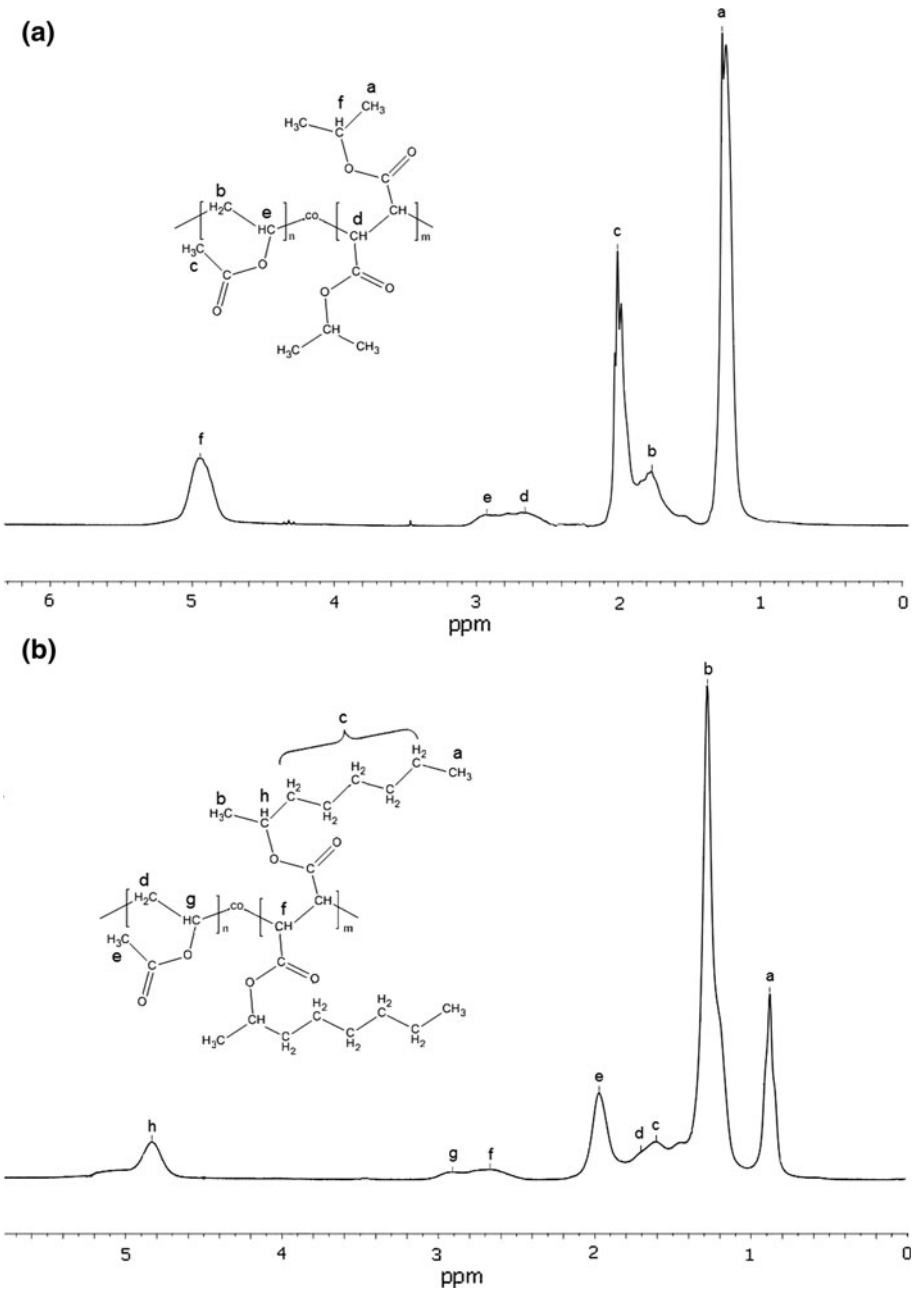

Fig. 1 ^{1}H NMR spectra in Cl_3DC at 40 °C: **a** Poly(VA-co-DIPF), **b** Poly(VA-co-DOF)

Table 1 Copolymerization of vinyl acetate (VA) and dialkyl fumarate (DRF), percent of conversion (Conv), weight average molecular weight (M_w) and polydispersity index (PDI) of copolymers synthesized

Copolymer	Time (min)	Conv (%)	F^{a}_{DRF}	M_w (kDa)[b]	PDI[b]	T_g (°C)
Poly(VA-co-DIPF)	15	58	0.40	287	1.9	39.3
Poly(VA-co-DOF)-1	4	28	0.37	419	5.5	16.2
Poly(VA-co-DOF)-2[c]	4	25	0.30	262	8.7	18.4

Reaction conditions using microwave energy: VA:DRF = 75:25, [BP] = 40 mM, power irradiation = 140 W

[a] F_{DOF} is the mole fraction of DRF in copolymer: DIPF and DOF are diisopropyl and dioctyl fumarate respectively

[b] Weight average molecular weight (M_w) and polydispersity index (PDI) determined by SEC according to the ratio M_w/M_n

[c] 0.01 mol.% dodecylmercaptan (CTA)

could be the result of two opposing effects: on the one hand, the decrease in M_w, by chain transfer reaction to CTA, which contributes to the soluble fractions and on the other, the formation of a non-crosslinked branched polymers fraction (high M_w), but soluble, through chain transfer reaction to polymers, as was indicated in Fig. 2.

Other important property of the polymers is the glass transition temperature (T_g). T_g is a characteristic temperature above which the mobility of the polymer chains is markedly increased. Transport properties depend on the free volume within the polymer and on the segmental mobility of the polymer chain, which influence on the mass transfer rates of water and drugs. Comparatively, polymers with low glass transition temperatures possess greater segmental mobility and will have higher diffusivity. The segmental mobility of the polymer chains depend of factor such as the extent of unsaturation, degree of crosslinking, degree of crystallinity, nature of substituents and average molecular weight.

In order to obtain information about this relevant aspect to future applications, the T_g of the copolymers were measurement and the results are present in the last column

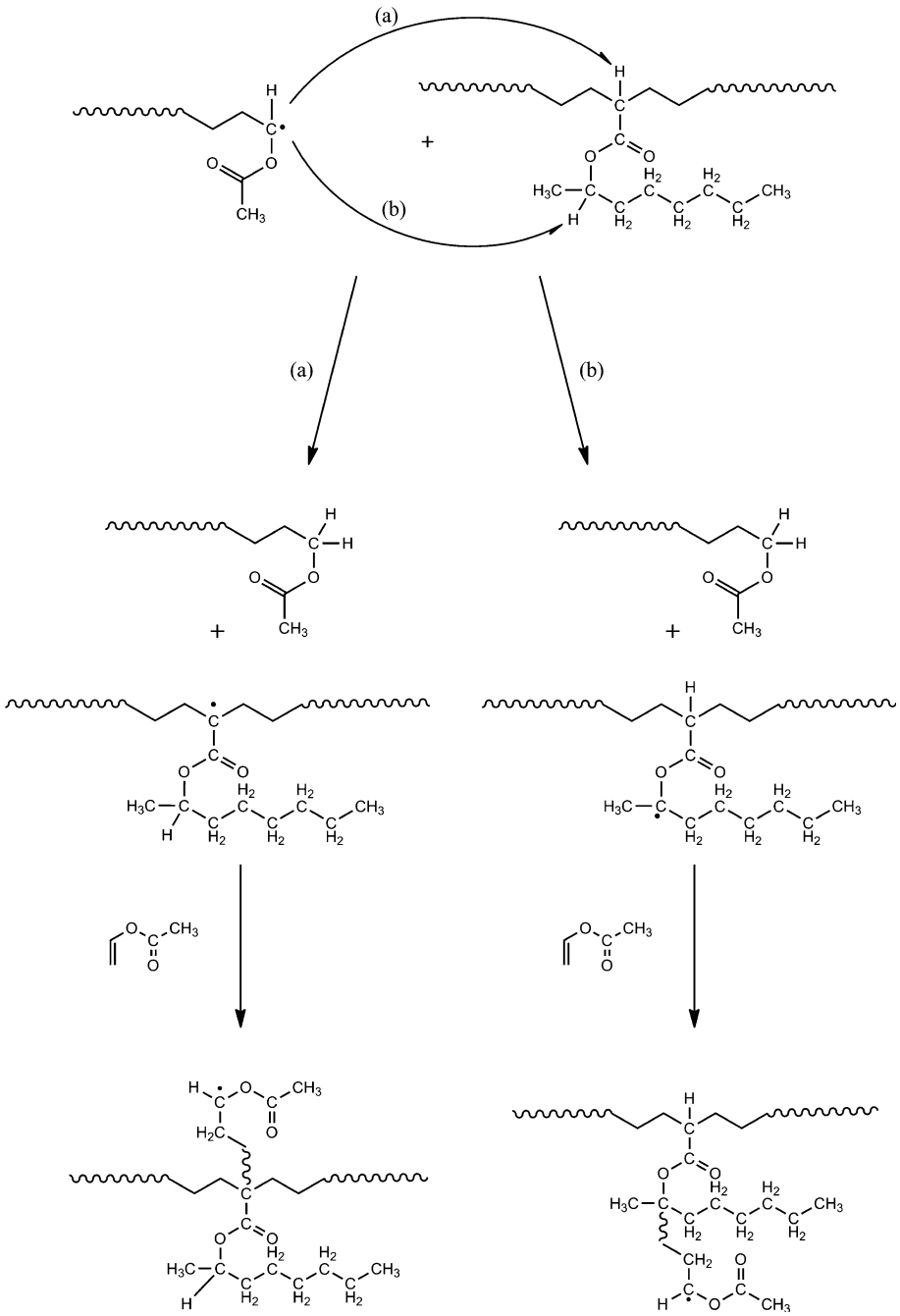

Fig. 2 Mechanisms of chain transfer to polymer in free-radical copolymerization of vinyl acetate and dioctyl fumarate

of the Table 1. The DIPF copolymer exhibited a T_g above room temperature, consistent with the chemical structure of the pendent substituent, while presented as a vitreous and brittle material, as was reported for others researches [34]. These characteristics led us to modify the chemical structure of copolymer by changing the length of the ester group, in order to obtain a macromolecule with a lowest T_g (highest free volume). In view of this goal DOF was synthesized and copolymerized with VA and the corresponding T_g values were below room temperature, as expected (see Table 1).

3.2 Membrane characterization

The membranes prepared by employing the two kinds of copolymers with thickness of 220 ± 20 μm were homogenous and highly transparent, as can be seen in Fig. 3. Transparency can be used as a criterion for determining the formation of homogeneous phase between PVA (backing layer) and poly(VA-co-DRF) components [35]. In addition, this property gives a good an esthetical appearance to film, an important consideration to contemplate for transdermal delivery system applications.

The SEM images of these membranes, depicted in Fig. 4, allow us to analyze the morphology and texture at the micrometer level. They have a dense and homogeneous microstructure, with a smooth texture superficial (Fig. 4a, c), but some irregularities appears on the poly(VA-co-DIPF) surface. Cross-sectional SEM images showed that phase separation is noteworthy for DIPF copolymer (Fig. 4b), while it is hardly appreciable for the DOF copolymer (Fig. 4d). These observations suggesting a good interaction between PVA and poly(VA-co-DOF) components, as anticipated based on the macroscopic characteristics of the membranes. The possible chemical interactions could be assigned to hydrogen bond between OH group of PVA and the carbonyl group present in copolymers. This kind of interactions may be favored in the poly(VA-co-DOF) due to the higher flexibility of the macromolecular chain, as a consequence of the large pendent group, which was confirmed by the low T_g (see Table 1). Poly(VA-co-DOF)-2 exhibited similar morphological characteristic than poly(VA-co-DOF)-1 (image not shown). These results indicating that the employed methodology was successful to obtain homogeneous membranes without large defects, such as pores or voids.

Fig. 3 Macroscopic appearance of the fumarate-based membrane: **a** Poly(VA-co-DIPF), **b** Poly(VA-co-DOF)-1

3.3 Mechanical properties

The applicability of polymeric film as TDD systems strongly depends on mechanical properties [36]. Table 2 shows the results for tensile properties of fumarate copolymers. It is possible to see that despite containing 60 mol.% of vinyl acetate, poly(VA-co-DIPF) is fairly inelastic and very brittle, similar to the homopolymer, as expressed by the moderate elastic modulus value (2 MPa) and low ultimate tensile stress. Yamada et al. [37], studied the mechanical properties of PDIPF in relationship to the molecular aggregation state, founded that the brittle fracture took place at 17–60 °C, while a large plastic deformation occurred at 110–200 °C. Comparatively, DOF copolymers (samples 1 and 2) exhibited lower elastic modulus value, without showing significant differences between them, in relation to the weight average molecular weight. Both copolymers are soft and tough materials, as evidence for a moderated ultimate tensile stress and high elongation at break [38]. The highest elongation at breaking point value found for poly(VA-co-DOF)-1, could be attributed to their highest M_w (see Table 1), as was previously demonstrated for other systems [39]. These results indicate that the DOF copolymers exhibited better mechanical properties that DIPF copolymer and they are promising candidates as membrane for TDD systems applications, according to the general properties suggested for such systems [18].

3.4 Swelling study

Taking into account before mentioned results we decided to carried out the swelling experiment on the poly(VA-co-DOF)-based membrane. Figure 5 shows the swelling behavior of both DOF copolymers, which differs on the M_w.

The curves show a rapid increase in the percentage of swelling up to 6–8 min and then reaching an equilibrium value (48.7 and 52.5 % for the copolymers 1 and 2, respectively). The observed differences could be attributed to the different M_w of the samples. As was indicated previously, the polymer molecular weight significantly influences the transport process [40]. As average molecular weight increases, the number of chain ends decreases; this chain ends represent a discontinuity and may form sites for permeant molecules to be sorbed into polymeric membrane.

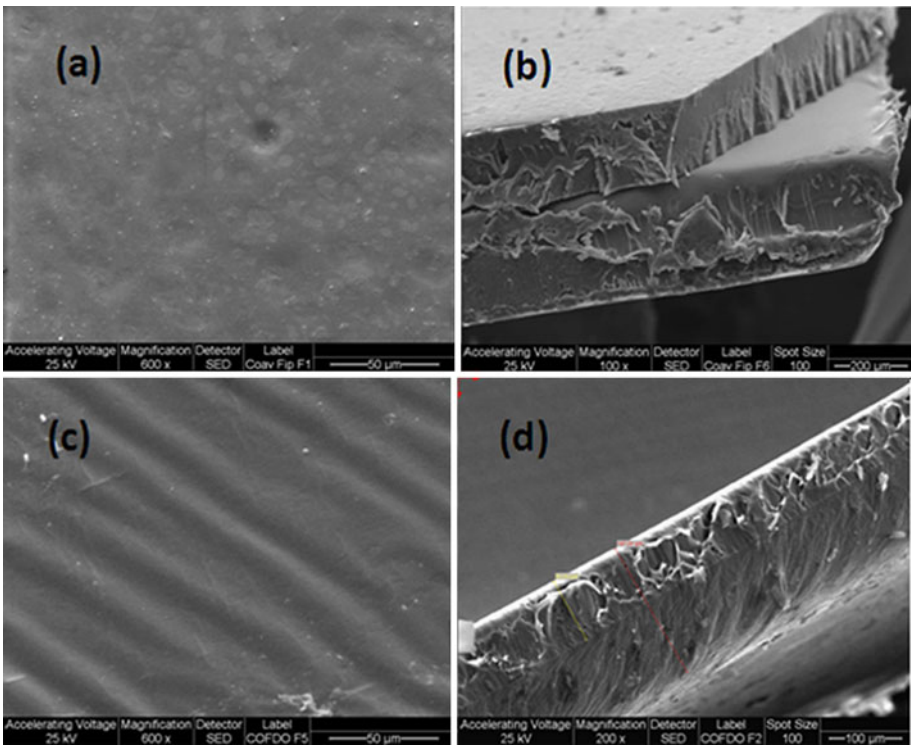

Fig. 4 SEM micrographs of surface and cross-sectional of poly(VA-co-DiPF) (**a** and **b**) and poly(VA-co-DOF)-1 (**c** and **d**), respectively

Table 2 Mechanical properties of poly(VA-co-DOF)

Copolymer	Elastic modulus[a] (MPa)	Ultimate tensile stress (MPa)	Elongation at breaking point (%)
Poly(VA-co-DIPF)	1.98 ± 0.19	3.10 ± 0.4	2.3 ± 0.3
Poly(VA-co-DOF)-1	1.11 ± 0.14	6.30 ± 1.1	111 ± 30
Poly(VA-co-DOF)-2	1.37 ± 0.20	10.25 ± 0.4	36 ± 7

[a] Values at 0.5–1.0 % of elongation

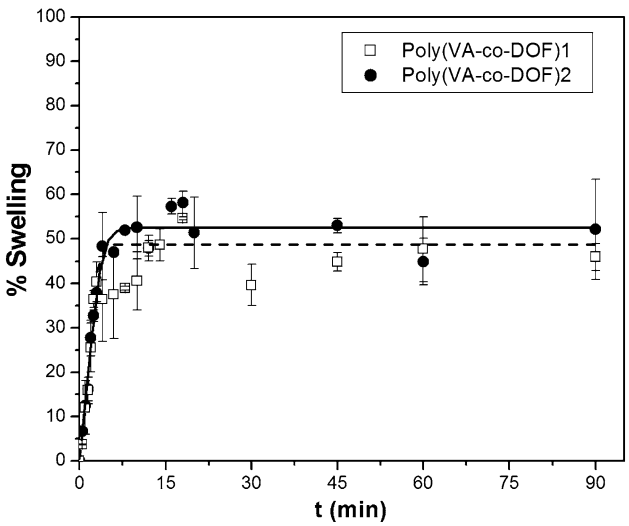

Fig. 5 Percentage of swelling of poly(VA-co-DOF) with different M_w as a function of time at 37 °C

No changes were observed in the dry weight of these membranes (w_d) during the 90 min of the swelling experiment. This observation indicate that the membrane were stable and do not suffer degradation process under the evaluated conditions.

Swelling is continuous process of transition from unsolvated glassy or partially rubbery state to a relaxed rubbery region [27]. During this process the water molecule diffuse into the polymer matrix acting as plasticizers and promote relaxation of the macromolecular chains. As mentioned previously, the kinetics of such process could be analyzed through the Fick model (Eq. 2) in order to determine the n exponent.

Figure 6 shows the linear regression plots of the fractional water absorbed at short times, according to Eq. (2). For the two membrane investigated the n values were very similar, 1.03 and 0.98 for the copolymers 1 and 2, respectively. These results suggest that the mechanism of water transport occur by a non-Fickian diffusion process, probably with rapid water diffusion in comparison to the macromolecular chain relaxation. Although DOF comonomer gives hydrophobicity to the copolymer, the long chain of this substituent decreases the T_g, increasing the free volume of the macromolecule, which could justify the rapid penetration of water. This study also helps to understand the behavior of environment's diffusion toward

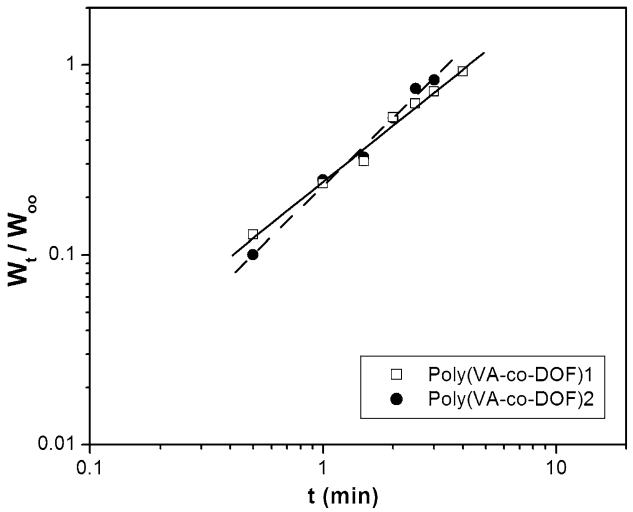

Fig. 6 Double logarithmic plot between W_t/W_∞ and time at initial stage

the inside of the membrane, as a preliminary test in drug delivery.

Studies of drug/polymer interaction and dermal release of bisphosphonate from poly(VA-co-DOF)-based membrane are at the present under progress in our laboratory.

4 Conclusions

Three new fumarate copolymers were prepared by microwave radical copolymerization, which differ in the nature of the moieties groups and the average molecular weight. The membrane obtained based of them have different properties, highlighting the importance of appropriate selection of the monomer to achieve the right properties to a TDD system. Poly(VA-co-DOF)-based membrane, are transparent, with good mechanical properties and exhibited a non-Fickian water transport mechanism, indicating that the release of a drug will be governed by the relaxation of the polymer chains.

Acknowledgments This work was supported by Universidad Nacional de La Plata (Project 11/X515). The authors are grateful to Fernando Amarilla for measuring the mechanical properties.

References

1. Shu KZ, Zhu KJ. The influence of multivalent phosphate structure on the properties of ionically cross-linked chitosan films for controlled drug release. Eur J Pharm Biopharm. 2002;54:235–43.
2. Khan Y, Yaszemski MJ, Mikos AG, Laurencin CT. Tissue engineering of bone: materials and matrix considerations. J Bone Joint Surg Am. 2008;90:36–42.
3. Kim HW, Knowles JC, Kim HE. Hydroxyapatite/poly(ε-caprolactone) composite coatings on hydroxyapatite porous bone scaffold for drug delivery. Biomaterials. 2004;25:1279–87.
4. Stamatialis DF, Papenburg BJ, Gironés M, Saiful S, Bettahalli SNM, Schmitmeier S, Wessling M. Medical applications of membranes: drug delivery, artificial organs and tissue engineering. J Membr Sci. 2008;308:1–34.
5. Ramachandran C, Fleisher D. Transdermal delivery of drugs for the treatment of bone diseases. Adv Drug Delivery Rev. 2000;42:197–223.
6. Chase JL. Lowering the risk of esophagitis from alendronate theraphy. Am J Health Syst Pharm. 1998;55:892–3.
7. Schenk R, Eggi DP, Fleisch DP, Rosini S. Quantitative morphometric evaluation of the inhibitory activity of new aminobisphosphonates on bone resorption in the rat. Calcif Tissue Int. 1986;38:342–9.
8. Gangoiti MV, Cortizo AM, Arnol V, Felice JI, McCarthy AD. Opposing effects of bisphosphonates and advanced glycation end-products on osteoblastic cells. Eur J Pharmacol. 2008;600:140–7.
9. Lin JH. Bisphosphonates: a review of their pharmacokinetic properties. Bone. 1996;18:75–85.
10. Josse S, Faucheux C, Soueidan A, Grimandi G, Massiot D, Alonso B, Janvier P, Laïb S, Pilet P, Gauthier O, Daculsi G, Guicheux J, Bujoli B, Bouler JM. Novel biomaterials for bisphosphonate delivery. Biomaterials. 2005;26:2073–80.
11. Oliveira AL, Pedro AJ, Arroyo CS, Mano JF, Rodriguez G, San Roman J, Reis RL. Biomimetic Ca–P coatings incorporating bisphosphonates produced on starch-based degradable biomaterials. J Biomed Mater Res B Appl Biomater. 2010;92:55–67.
12. Choi A, Ganga H, Chunb I, Gwak H. The effects of fatty acids in propylene glycol on the percutaneous absorption of alendronate across the excised hairless mouse skin. Int J Pharm. 2008;357:126–31.
13. Kusamori K, Katsumi H, Abe M, Ueda A, Sakai R, Hayashi R, Hirai Y, Quan YS, Kamiyama F, Sakane T, Yamamoto A. Development of a novel transdermal patch of alendronate, a nitrogen-containing bisphosphonate, for the treatment of osteoporosis. J Bone Miner Res. 2010;25:2582–91.
14. Nam SH, Xu YJ, Nam H, Jin GW, Jeong Y, An S, Park JS. Ion pairs of risedronate for transdermal delivery and enhanced permeation rate on hairless mouse skin. Int J Pharm. 2011;419:114–20.
15. Funke AP, Günther C, Müller RH, Lipp R. Development of matrix patches for transdermal delivery of a highly lipophilic antiestrogen. Drug Dev Ind Pharm. 2003;29:785–93.
16. Taghizadeh SM, Soroushnia A, Mirzadeh H, Barikani M. Preparation and in vitro evaluation of a new fentanyl patch based on acrylic/silicone pressure-sensitive adhesive blends. Drug Dev Ind Pharm. 2009;35:487–98.
17. Snorradóttir BS, Gudnason PI, Thorsteinsson F, Másson M. Experimental design for optimizing drug release from silicone elastomer matrix and investigation of transdermal drug delivery. Eur J Pharm Sci. 2011;42:559–67.
18. Tan HS, Pfister WR. Pressure-sensitive adhesives for transdermal drug delivery systems. Pharm Sci Technol Today. 1999;2:60–9.
19. Cortizo MS, Molinuevo MS, Cortizo AM. Biocompatibility and biodegradation of polyesters and polyfumarates based-scaffold for bone tissue engineering. J Tissue Eng Regen Med. 2008;2:33–42.
20. Fernandez JM, Molinuevo MS, Cortizo AM, McCarthy AD, Cortizo MS. Characterization of poly-ε-caprolactone/polyfumarate blends as scaffolds for bone tissue engineering. J Biomater Sci Polym Ed. 2010;21:1297–312.
21. Fernandez JM, Molinuevo MS, Cortizo MS, Cortizo AM. Development of an osteoconductive PCL-PDIPF-hydroxyapatite

composite scaffold for tissue engineering. J Tissue Eng Regen Med. 2011;5:126–35.
22. Cortizo MS. Polymerization of diisopropyl fumarate under microwave irradiation. J Appl Polym Sci. 2007;103:3785–91.
23. Oberti TG, Alessandrini JL, Cortizo MS. Thermal characterization of novel *p*-nitrobezylacrylate-diisopropyl fumarate copolímero synthesized under microwave energy. J Therm Anal Calorim. 2012;109:1525–31.
24. Mukherjee B, Mahapatra S, Gupta R, Patra B, Tiwari A, Arora P. A comparison between povidone-ethylcellulose and povidone-eudragit transdermal dexamethasone matrix patches based on in vitro skin permeation. Eur J Pharm Biopharm. 2005;59: 475–83.
25. Cortizo MS, Alessandrini JL, Etcheverry SB, Cortizo AM. A vanadium/aspirin complex controlled release using a poly(β-propiolactone) films. Effect on osteosarcoma cells. J Biomater Sci Polym Ed. 2001;12:945–59.
26. Ritger L, Peppas NA. A simple equation for description of solute release. I. Fickian and non-Fickian release from non-swellable devices in the form of slabs, spheres, cylinders or discs. J Control Release. 1987;5:23–6.
27. Ganji F, Vasheghani-Farahani S, Vasheghani-Farahani E. Theoretical description of hydrogel swelling: a review. Iran Polym J. 2010;19:375–98.
28. Otsu T, Matsumoto A, Shiraishi K, Amaya N, Koinuma Y. Effect of the substituents on radical copolymerization of dialkylfumarates with some vinyl monomers. J Polym Sci Part A. 1992;30: 1559–65.
29. Al-Arbash AH, Elsagheer FA, Ali AAM, Elsabee MZ. Glass-transition temperature of polydialkyl fumarate copolymers. J Polym Sci Part A. 1999;37:1839–45.
30. Otsu T, Minai H, Toyoda N, Yasuhara T. Radical high polymerization of dialkylfumarates with bulky substituents leading to less-flexible rod-like polymers. Die Makromol Chem Suppl. 1985;12:133–42.
31. Britton D, Heatley F, Lovell PA. Chain transfer to polymer in free-radical bulk and emulsion polymerization of vinyl acetate studied by NMR spectroscopy. Macromolecules. 1998;31: 2828–37.
32. Heatley F, Lovell PA, Yamashita T. Chain transfer to polymer in free-radical solution polymerization of 2-ethylhexyl acrylate studied by NMR spectroscopy. Macromolecules. 2001;34:7636–41.
33. Gonzalez I, Asua JM, Leiza JR. The role of methyl methacrylate on branching and gel formation in the emulsion copolymerization of BA/MMA. Polymer. 2007;48:2542–7.
34. Koinuma Y, Murata Y, Otsu T, Goto K, Fujiwara H, Takita Y. Thermal and mechanical properties of poly(diisopropyl fumarate) blends with various polymers. Kobunshi Ronbunshu. 1997;54: 301–8.
35. Aparicio M, Duran A. Hybrid organic/inorganic sol–gel materials for proton conducting membranes. J Sol Gel Sci Technol. 2004; 31:103–7.
36. Guo R, Du X, Zhang R, Deng L, Dong A, Zhang J. Bioadhesive film formed from a novel organic–inorganic hybrid gel for transdermal drug delivery system. Eur J Pharm Biopharm. 2011; 79:574–83.
37. Yamada K, Takayanagi M, Murata Y. Relations between molecular aggregation state and mechanical properties in poly(diisopropyl fumarate). Polymer. 1986;27:1054–7.
38. Aulton ME, Abdul-Razzak MH, Hogan JE. The mechanical properties of hydroxyl propyl methyl cellulose films derived from aqueous systems: the influence of solid inclusions. Drug Dev Ind Pharm. 1981;7:649–68.
39. Flory PJ. Tensile strength in relation to molecular weight of high polymers. J Am Chem Soc. 1945;67:2048–50.
40. George SC, Thomas S. Transport phenomena through polymeric systems. Prog Polym Sci. 2001;26:985–1017.